Astron. Astrophys. 351, 937–944 (1999)

ASTRONOMY AND ASTROPHYSICS

X-ray spectral components from a broad band BeppoSAX observation of the Seyfert galaxy IC 4329A

G.C. Perola[1], G. Matt[1], M. Cappi[2], D. Dal Fiume[2], F. Fiore[3], M. Guainazzi[4], T. Mineo[5], S. Molendi[6], F. Nicastro[7], L. Piro[8], and G. Stirpe[9]

[1] Dipartimento di Fisica, Università degli Studi "Roma Tre", Via della Vasca Navale 84, 00146 Roma, Italy
[2] Istituto Tecnologie e Studio Radiazioni Extraterrestri, CNR, Via Gobetti 101, 40129 Bologna, Italy
[3] Osservatorio Astronomico di Roma, Via dell'Osservatorio, 00044 Monteporzio Catone, Italy
[4] Astrophysics Division, Space Science Department of ESA, ESTEC, Postbus 299, 2200 AG Noordwijk, The Netherlands
[5] Istituto di Fisica Cosmica ed Applicazioni all'Informatica, C.N.R., Via U. La Malfa 153, 90146 Palermo, Italy
[6] Istituto di Fisica Cosmica "G. Occhialini", C.N.R., Via Bassini 15, 20133 Milano, Italy
[7] Harvard-Smithsonian Center for Astrophysics, 60 Garden st., Cambridge, MA 02138, USA
[8] Istituto di Astrofisica Spaziale, C.N.R., Via Fosso del Cavaliere, 00133 Roma, Italy
[9] Osservatorio Astronomico di Bologna, Viale Berti Pichat 6/2, 40127 Bologna, Italy

Received 11 May 1999 / Accepted 27 September 1999

Abstract. From the spectral analysis of a broadband (0.1–200 keV) BeppoSAX observation of the Seyfert 1 galaxy IC 4329A, the main results obtained are: a) the amount of reflection, together with the intensity of the iron K line, indicate a geometry with a solid angle substantially less than 2π; b) the power law is affected by a cut off with e-folding energy about 270 keV, the fourth individual object so far where this property has been firmly detected; c) two absorption features at about 0.7 and 1 keV are found, the first corresponding to a blend of O VI and O VII, the other to a combination of FeL and NeK edges. Compared to an earlier ASCA observation, when the source was 30% fainter, the values of both the relative amount of reflection and the warm absorber ionization degree are significantly lower: the comparison is suggestive of sizeable delay effects in this object, due to geometrical factors in the reflection, and to relaxation to equilibrium states in the ionization of the absorber.

Key words: galaxies: individual: IC 4329A – galaxies: Seyfert – X-rays: galaxies

1. Introduction

Starting from EXOSAT and Ginga observations, it has become progressively clear that the X–ray spectra of Seyfert 1 galaxies are rather complex (see, e.g., Mushotzky et al. 1993, and ref. therein), with the effects of radiative transfer in the environment of the central engine complicating the view of the primary emission. The latter is empirically described as a power law, which, according to OSSE/CGRO observations (Gondek et al. 1996, Zdziarski et al. 1995), appears to break at high energies in a manner that can be described to a first approximation by an exponential cutoff, although the value of the e-folding energy in individual objects remains to be properly constrained. At energies below about 1–2 keV the incidence of a further continuum component in excess to the power law, the so–called soft X–ray excess, is not yet completely well assessed, with ASCA data showing it to be rather less common (e.g. Reynolds 1997) than in ROSAT data (e.g. Walter & Fink 1993). In fact this issue had a significant turn after the discovery with ROSAT and, more accurately, with ASCA of the rather common incidence of a warm absorber: in essence, both types of features are determined with less ambiguity the better the slope of the power law is constrained, a task which ASCA, in addition to the higher energy resolution, could achieve more directly than ROSAT because of its energy coverage up to 10 keV. To complicate the matter there is another, seemingly ubiquitous, continuum component, which affects the power law slope determination in the ASCA band (as it previously did in the HEAO1 and EXOSAT bands) and peaks beyond that band, around 30 keV. This component, discovered with Ginga, is interpreted as Compton reflection of the power law photons off thick matter that can be the accretion disk itself and/or the torus envisaged in the unified Seyfert 1 and 2 scenario. This component is typically accompanied by the iron K fluorescence line, discovered in fact before the reflection. The accuracy achieved on the strength of the reflection is then relevant to the determination of the power law slope and, consequently, of the soft excess and/or the warm absorber parameters. Observationally the situation is further complicated by the well known variability of these objects, such that combining data from satellites covering different energy ranges, and collected at different times, leads to further ambiguities.

The Narrow Field Instruments aboard BeppoSAX offer for the first time the opportunity to cover simultaneously, and with a reasonably good spectral resolution, the band from 0.1 to 200 keV, hence to determine the various spectral parameters,

Send offprint requests to: G.C. Perola (perola@fis.uniroma3.it)

especially the broad ones, with better confidence than could be done before. This paper reports results obtained as part of a broad band spectral survey of Seyfert 1s, with 2–10 keV fluxes greater than about 1–2 mCrab. After the observation of NGC 4593 described in Guainazzi et al. (1999a) here we present the observation of the brightest source in the sample, IC 4329A. In Sect. 2 the earlier X–ray studies are summarized. In Sects. 3 and 4, the data reduction and the spectral analysis are respectively presented. In Sect. 5 these results are commented on and compared with previous ones, and the conclusions are drawn in Sect. 6.

2. IC 4329A in X–rays

IC 4329A is classified as a Seyfert 1.0 galaxy (Whittle 1992) at z=0.016 (Wilson & Penston 1979). The 2–10 keV flux records in the literature show a relatively modest variability on timescales of hours–days, and fall within 50% of 1.0×10^{-10} erg cm^{-2} s^{-1} (corrected for absorption), corresponding to L(2–10 keV) = 10^{44} erg s^{-1} (H_0=50 km s^{-1} Mpc^{-1}). However, from inspection of the 2–10 keV light curve from the ASM instrument onboard Rossi XTE (quick look results provided by the ASM/RXTE team) it appears that this object undergoes occasional outbursts by up to a factor of about 10, with timescales of the order of a few days. Furthermore a factor 3 decline in about four days in visible in the light curve from the January 1993 OSSE/CGRO observation, albeit in the quite different band from 50 to 150 keV (Fabian et al. 1993).

The spectrum displays neutral absorption at low energies, due to a gas column about ten times greater than the galactic value N_{Hg}=4.5×10^{20} cm^{-2} (Elvis et al. 1989), conceivably associated with the disk of the host galaxy, which is oriented nearly edge–on (Petre et al. 1984).

This object is one of the first AGN where a reflection component was individually detected with Ginga (July 8–10 1989 observation; Piro et al. 1990, Nandra & Pounds 1994): the amplitude of this component relative to the power law was found to be roughly consistent with an $\Omega=2\pi$ slab of reflecting matter, and the intensity of the iron K line simultaneously measured had EW$\simeq$110 eV from a gaussian fit. A time resolved spectral analysis of the same data by Fiore et al. (1992) presents tentative evidence of a time lag by more than three days in the response of the reflection component to an increase of the power law by 20% in three days. Contemporaneous observations with ROSAT and OSSE/CGRO in January 1993 (Madejski et al. 1995) gave for the reflection component results, with large errors, consistent with those obtained by Ginga, providing in addition a lower limit of about 100 keV for the e–folding energy of the power law. The August 15 1993 ASCA observation has been analyzed in several papers (Mushotzky et al. 1995, Cappi et al. 1996, Nandra et al. 1997, Reynolds 1997, George et al. 1998). The detailed analysis by Cappi et al. (1996), for what concerns the reflection, provides results surprisingly at variance with those obtained with Ginga: despite the flux level being only 30% lower, the best fit relative normalization of the reflection component is about three times stronger, while the gaussian fit of the iron line yields about the same EW (89$\pm$34 eV at 90% confidence for one interesting parameter, i. p.). This result is hard to reconcile with the idea that both the line and the reflection arise from the same matter, and we shall return to it in Sect. 5.

At low energies Madejski et al. (1995) discovered with ROSAT the existence either of the ionized edge imprinting by an additional warm absorber, or of a soft excess. The ambiguity was convincingly resolved by Cappi et al. (1996), who found in the ASCA data evidence of two rather strong edges, one consistent with O VII, the other with O VIII (this aspect is investigated also in Reynolds 1997 and George et al. 1998, see Sect. 5).

3. Observations, data reduction and temporal analysis

A general description of the Italian–Dutch satellite BeppoSAX can be found in Boella et al. (1997a). The observations were made with the four, coaligned Narrow Field Instruments: the two imaging instruments covering, respectively, the band 0.1–10 keV (LECS, Low Energy Concentrator Spectrometer, Parmar et al. 1997) and the band 1.8–10.5 keV (MECS, Medium Energy Concentrator Spectrometer, Boella et al. 1997b); the two collimated instruments, covering respectively the band 4–120 keV (HPGSPC, High Pressure Gas Scintillation Proportional Counter, Manzo et al. 1997) and the band 13–200 keV (PDS, Phoswich Detector System, Frontera et al. 1997), with their collimators operating in the rocking mode (time–on = time–off = 96 s) to monitor the background throughout the observation. The data from the HPGSPC, an instrument tuned for spectroscopy of very bright sources, provided in our case barely significant constraints and will therefore not be considered in this paper. Due to rather subtle problems that remain in the exploitation for spectral analysis of LECS data above 4 keV, we shall use only data in the range 0.1–4.0 keV.

In Table 1 the start date of the observation, the net exposure times and the net average count rates are given. The exposure time in the LECS is much shorter than in the MECS because the former instrument is operated only during the night–time fraction of each orbit. The reduction procedures and screening criteria used to produce the linearized and (between the two MECS units) equalized event files are standard and have been described in Guainazzi et al. (1999a). In particular, of the two options available for the PDS, we used the Rise Time selection criterion.

The spectral counts in the imaging instruments were extracted from circular regions of radius 4 arcmin (MECS) and 8 arcmin (LECS) around the source centroid, and the background subtraction was performed using spectra from blank sky event files in the same position of the detectors. The background count rate used is 2.74×10^{-2} c s^{-1} in the LECS, 6.95×10^{-3} c s^{-1} (2 units) in the MECS, and the error on the net counts (in Table 1) is dominated by the source statistics. Spectra and light curves from the PDS were obtained from direct subtraction of the off– from the on–source products, and the error on the net counts (in Table 1) is dominated by the background statistics.

In the field of view of the PDS, 1.3° FWHM, care must be taken of sources that could contaminate the target signal.

Table 1. Observation epoch and mean count rates. The count rate for the MECS refers to two units

Start date	LECS	LECS	MECS	MECS	PDS	PDS
	t_{exp} s	CR (0.1–10 keV) cts s^{-1}	t_{exp} s	CR (1.8–10.5 keV) cts s^{-1}	t_{exp} s	CR (13–200 keV) cts s^{-1}
1998-Jan-02 (9h 1m 16s UT)	25097	0.696±0.005	81826	1.551±0.004	75214	0.983±0.015

Table 2. Hardness ratios: mean values and χ^2 for a constant value

HR($\frac{1.8-4}{0.1-1.8}$)[a]	χ^2_ν/d.o.f.	HR($\frac{4-10.5}{1.8-4}$)[b]	χ^2_ν/d.o.f.	HR($\frac{13-100}{1.8-10.5}$)	χ^2_ν/d.o.f.
1.04	1.27/28	0.74	0.83/28	0.61	1.31/28

[a] based on LECS data only
[b] based on MECS data only

IC 4329A belongs to the cluster of galaxies A 3574, which is a comparatively very weak X–ray emitter (Pierre et al. 1994). We integrated its surface brightness in the ROSAT pointed observation described in Madejski et al. (1995) to obtain a rough estimate of the flux: in the 2–10 keV range (with an hypothetically large value of the temperature, kT=7 keV) it is about 30 times lower than that of IC 4329A, hence its contribution in the PDS is totally negligible. The same conclusion holds for the point source named S3 by Madejski et al. (1995), which lies at about 12 arcmin from the target, and that we find in the MECS image with a 2–10 keV flux of about 8.4×10^{-13} erg cm^{-2} s^{-1}, more than 100 times fainter than IC 4329A. Another source, associated with the elliptical galaxy IC 4329 located only 3 arcmin away from IC 4329A, might contaminate the signal of our target extracted from the LECS. Madejski et al. (1995) attribute to this source a thermal plasma spectrum with kT=0.87 keV, and a flux 6.5×10^{-13} erg cm^{-2} s^{-1} in the 0.1–2 keV range: from Fig. 6 of their paper we expect the contamination by this source to be possibly relevant only below 0.4 keV (but see Sect. 4).

The detailed study of the observed time variability goes beyond the scope of this paper, but some information is presented to justify the spectral analysis of the integrated spectra. Fig. 1 illustrates light and hardness ratio (HR) curves. The object underwent important intensity variations, but the χ^2 test applied to the strings of HR values (Table 2) shows that the evidence of deviations from a constant value is marginal overall: we conclude that spectral variations are unlikely to introduce, in the analysis on the integrated counts, an important bias in the estimate of the parameters. We shall, though, take care of the inhomogeneity in the time coverage between LECS and MECS, by letting the relative normalization of the two instruments as a free parameter. The normalization of the PDS to the MECS will instead be held fixed.

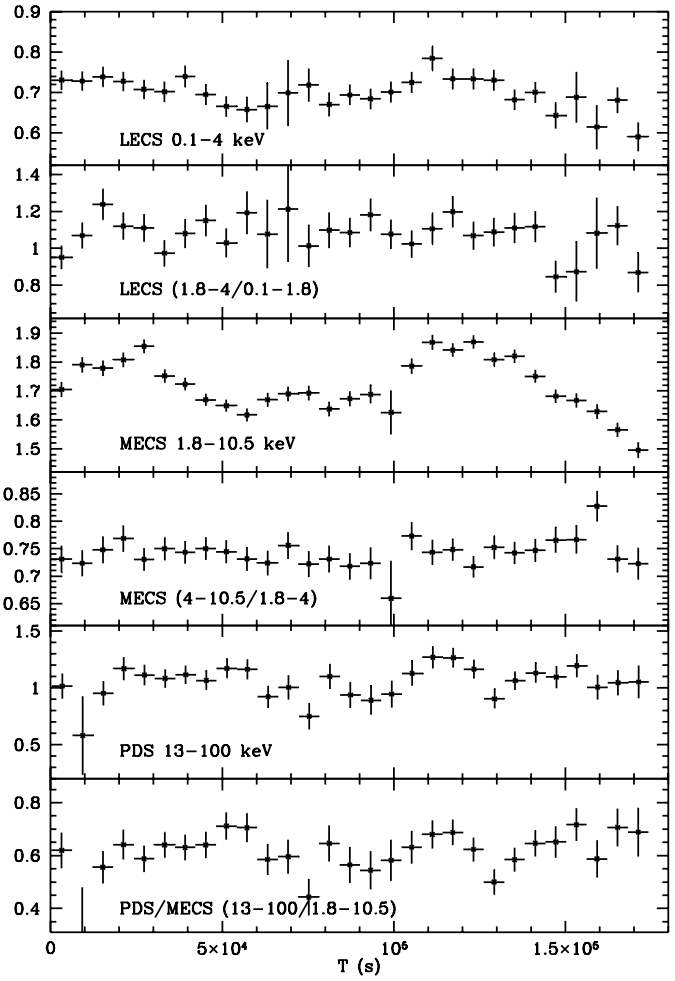

Fig. 1a–f. Light and HR curves of the IC 4329A observation, in time bins of 6000 s. **a** Light curve in the 0.1–4.0 keV LECS band and **b** HR(1.8–4.0/0.1–1.8). **c** Light curve in the 1.8–10.5 keV MECS band and **d** HR(4.0–10.5/1.8–4.0). **e** Light curve in the 13–100 keV PDS band and **f** HR(13–100/1.8–10.5). The LECS and MECS light curves are not background subtracted.

4. Spectral analysis

The analysis of the integral spectral counts was performed using the software package XSPEC (version 10). In the first step a "Baseline Model Spectrum" (BMS) was adopted, which is composed of: a Power Law with an exponential cut off (PL), described by three parameters, the normalization A, the photon index Γ and the e–folding energy E_f ($A\times E^{-\Gamma}\times\exp(-E/E_f)$); a Reflection Component (RC) with two parameters, $r=\Omega/2\pi$,

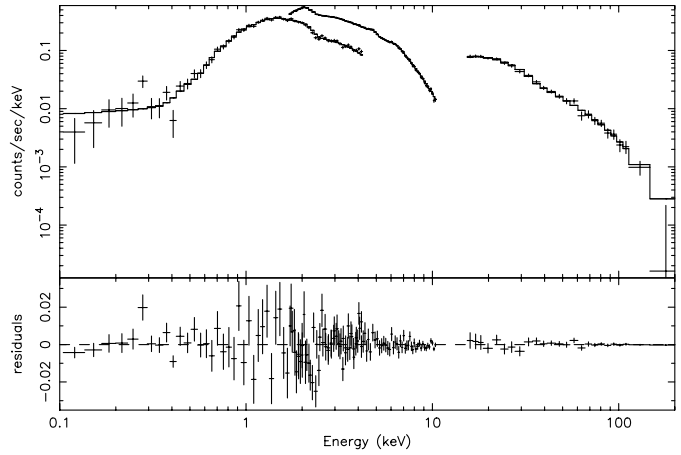

Fig. 2. LECS, MECS and PDS spectra with the best fit Baseline Model Spectrum (upper panel), and residuals (lower panel).

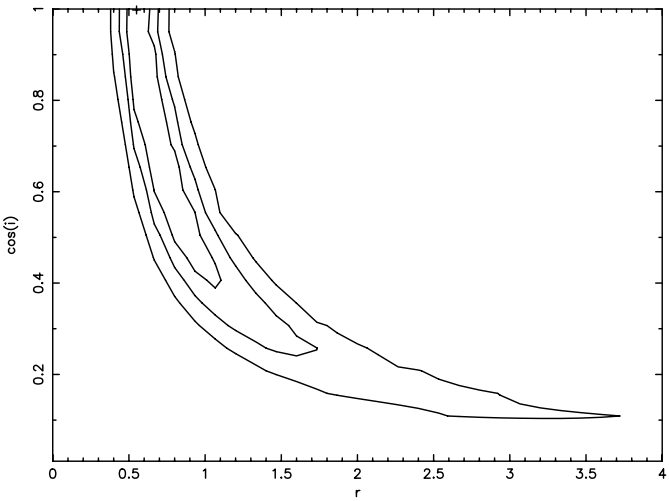

Fig. 3. Confidence (67, 90 and 99%) contours of the parameters r and cos i, when the inclination angle is a free parameter in the BMS fit.

the solid angle fraction of a neutral, plane parallel slab illuminated by the PL photons, and i, its inclination angle to the line of sight (module PEXRAV for PL and RC together); a uniform neutral column of gas in photoelectric absorption, N_H, in addition to the adopted value of the galactic N_{Hg} (module WABS; in both the slab and the column the element abundances used are the cosmic values in Anders & Grevesse 1993); a gaussian iron K line, with three parameters, E_k, σ_k and the intensity I_k, also given as an EW. Following the procedure adopted by Cappi et al. (1996), we included in the model also two absorption edges, with four parameters, their energies, E_1 and E_2, and maximum optical depths, τ_1 and τ_2.

The energy bins chosen represent about one third of the instrumental resolution, which is a function of the energy. The normalization C of the PDS relative to the MECS was adopted equal to 0.8 (Fiore et al. 1999). The "statistical" errors have been obtained holding C fixed at this value, and correspond to the 90% confidence interval for two i. p., or $\Delta\chi^2$=4.61. The "systematic" errors linked to the current $\pm$10% uncertainty on C will also be investigated.

The energies of the iron line and of the absorption edges are reported as in the rest frame of the host galaxy.

4.1. The BMS fit

The BMS fit was performed on the spectral counts from the three instruments together. The results are given in Table 3 and illustrated in Fig. 2. According to the χ^2 statistics, the BMS lies above an acceptability limit of 10%. Moreover, if the contribution to the χ^2 from the LECS points in the interval common to the MECS, 1.8–4 keV, is subtracted, it improves dramatically to 115.9/118. We see no evidence in the residuals of a significant contribution by IC 4329 below 0.5 keV.

Due to the weak dependence of the RC shape on cos i, the inclination angle is very poorly constrained, and consequently also the value of r, as shown in the confidence contour plots in Fig. 3: the best fit value of the angle is practically 0°, while the 90% upper limit read from the graph is about 70°. Lacking an objective independent estimate of this angle (but see Sect. 4.2), we adopt as a reference the face–on configuration for the best fit BMS results, as given in Table 3.

Table 3. Baseline Model Spectrum fit with cos i=1

F(2–10 keV)[a]	13.17$\pm$0.04
A[b]	4.16
Γ	$1.86^{+0.03\ (+0.03)}_{-0.03\ (-0.02)}$
N_H (10^{21} cm^{-2})[c]	$3.31^{+0.26\ (+0.22)}_{-0.50\ (-0.08)}$
E_f (keV)	$270^{+167\ (+70)}_{-80\ (-40)}$
r	$0.55^{+0.15\ (+0.27)}_{-0.13\ (-0.20)}$
E_k (keV)[d]	$6.48^{+0.17}_{-0.16}$
σ_k (keV)	$0.36^{+0.27}_{-0.21}$
I_k (10^{-4} cm^{-2} s^{-1})	$1.57^{+0.73\ (+0.12)}_{-0.59\ (-0.21)}$
EW_k (eV)	$109^{+50\ (+8)}_{-41\ (-14)}$
E_1 (keV)[d]	$0.73^{+0.44}_{-0.10}$
τ_1	$0.52^{+0.45}_{-0.37}$
E_2 (keV)[d]	$1.03^{+0.15}_{-0.13}$
τ_2	$0.19^{+0.16}_{-0.14}$
χ^2/d.o.f.	159.9/141

[a] As observed in 10^{-11} erg cm^{-2} s^{-1}
[b] In 10^{-2} cm^{-2} s^{-1} keV^{-1}
[c] In addition to N_{Hg}=4.55$\times10^{20}$ cm^{-2}
[d] In the source frame

Despite the uncertainty on the angle, the evidence of a RC is remarkably clear. However, the skewed shape of the confidence contours for the couple of parameters r and Γ (Fig. 4) shows that, despite the ample spectral coverage, the two parameters remain statistically correlated, and that the fractional uncertainty on r is more sensitive to the correlation than the one on Γ.

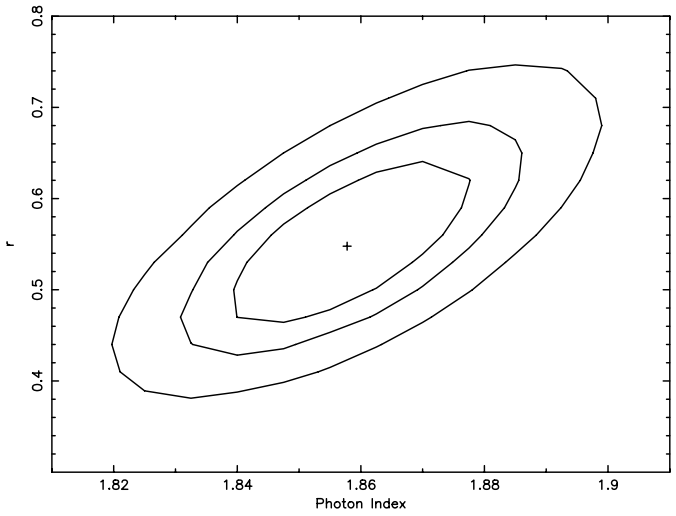

Fig. 4. Confidence (67, 90 and 99%) contours of the parameters Γ and r, in the BMS fit with cos i set equal to 1.

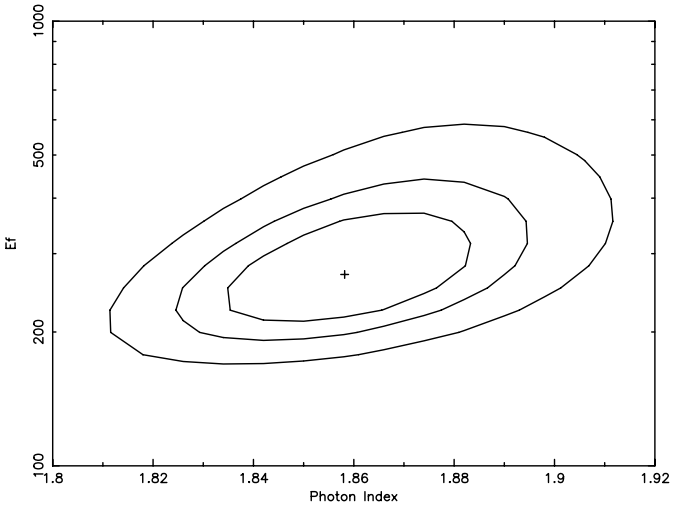

Fig. 5. Confidence (67, 90 and 99%) contours of the parameters Γ and E_f, in the BMS fit with cos i set equal to 1.

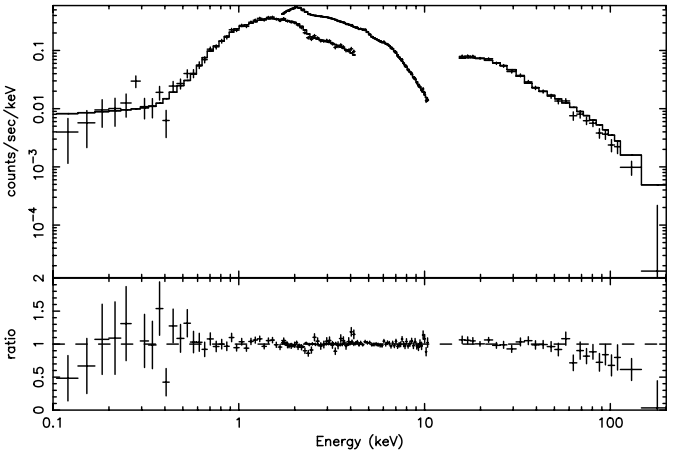

Fig. 6. LECS, MECS and PDS spectra with the best fit BMS without the exponential cutoff (upper panel), and ratio of data to model (lower panel).

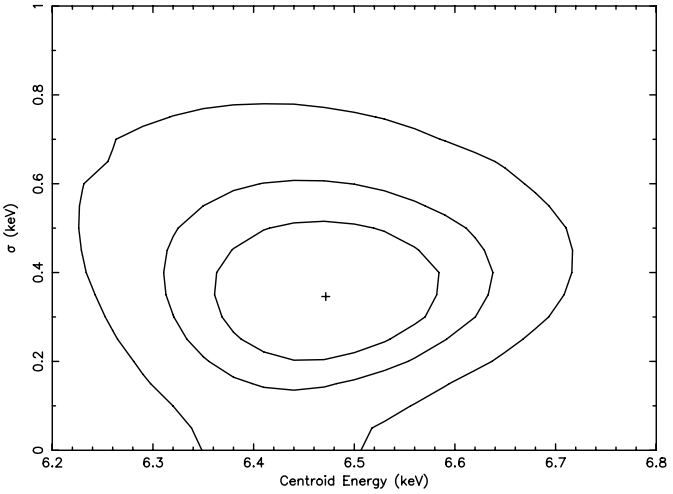

Fig. 7. Confidence (67, 90 and 99%) contours of the width (σ_k) and energy (E_k) of the iron line, in the BMS fit with cos i set equal to 1. The line energy is given in the frame of the host galaxy.

The next remarkable result is the evidence of the exponential cut–off, with rather tight constraints on the energy E_f. This is illustrated in Fig. 5, with the confidence contours of the two parameters Γ and E_f. When the BMS is fitted without the cut–off (Fig. 6), the residuals above 50 keV show a clear curvature, and the χ^2 is much larger, $\Delta\chi^2$=40: according to the F–test, this difference implies a probability less than 10^{-3} that the cut–off is due to random fluctuations in the counts. Notably the two broad band parameters Γ and r turn out practically the same in the two fits, thus showing that the estimate of E_f is quite well and independently constrained.

The confidence contours for the energy and width of the iron K line in Fig. 7 show that the line energy is consistent with the neutral value and that the line appears resolved (see Sect. 4.2).

The detection of two edges at about 0.7 and 1 keV confirms the presence of a warm absorber, whose physical state will be further analyzed in Sect. 4.3.

Finally we consider the systematic errors associated with the current uncertainty on the value of the PDS to MECS relative normalization, C, mentioned above. The parameters which are significantly affected by this uncertainty are N_H, Γ, E_f, r and the iron line intensity and EW. For these parameters, in Table 3, in addition to the statistical errors from the BMS fit, we give in parentheses the systematic error estimated from the best fit values obtained when C is set at 0.72 and 0.88. Notably, while for N_H, E_f, I_k and EW the systematic errors are comparatively small, this is not the case for r, where these errors are larger than the statistical errors, and for Γ, where they are comparable.

4.2. Further modelling of the iron K line

The line width is at least three times larger than in the optical emission lines (Wandel et al. 1999), and is suggestive of an origin from the accretion disk. In this case it is more natural to

replace the gaussian with the relativistic profile, as described in the module DISKLINE in XSPEC, where a Schwarzschild black hole is adopted. In doing that we fixed the line emission energy at 6.4 keV, the innermost radius at 6 times $R_g=GM/c^2$, i.e. the innermost stable orbit, the exponent of the radial dependence of the emissivity at β=–2 (the use of somewhat different values, such as β=–2.5, the average inferred by Nandra et al. 1997, on a large sample of objects, leads to very similar results). The free parameters are the intensity I_k, the outer radius, R_{out} in units of R_g, of the disk region contributing to the line and the inclination angle; under the assumption that most of the RC comes from the same matter, we required the angle to be the same for the two spectral components, hence this modification of the model leaves the number of free parameters unchanged with respect to the BMS fit with the angle fixed at 0° given in Table 3.

The fit with this model gives a χ^2 identical to the fit with the BMS, and the inclination angle turns out to be $49^\circ_{-8}{}^{+29}$ (notably smaller than that of the galaxian disk). The line parameters are $R_{out}>158$, $I_k=(1.63^{+0.71}_{-0.59})\times10^{-4}$ cm^{-2} s^{-1}, corresponding to $EW_k=118^{+51}_{-43}$ eV. Compared to the BMS fit results, the values of the other parameters in common are practically the same, except for the best fit value of r, which, as a consequence of the inclination angle being much larger than 0°, turns out to be somewhat greater, $r=0.72^{+1.23}_{-0.18}$.

One further fit comprises the addition of a narrow line at 6.4 keV to the previous model, with the intensity of this line being then the only additional parameter. This addition leads to a marginally significant decrease in chi square, $\Delta\chi^2$=–3.7 (93% significance, F–test), with the detection of a weak narrow line of $EW_{kn}=45^{+27}_{-31}$ eV. The parameters of the diskline become $R_{out}<43$, $EW_k=103^{+56}_{-65}$ eV, the inclination angle $i=45^\circ_{-6}{}^{+7}$, the reflection normalization $r=0.72^{+0.23}_{-0.18}$, the others remain practically unchanged (the upper 90% confidence bound on r is much smaller than in the previous fit because of the substantial reduction of the corresponding bound on the angle).

If the gas with the observed N_H completely surrounded the source, the EW of the associated narrow fluorescence line would be lower than observed by a factor about 10 and in order to match the observed value the iron abundance should be higher than normal by about the same factor. It is more plausible that the narrow line is produced in thicker neutral matter at the outskirts or outside the accretion disk, which should contribute also to the reflection continuum. If we assume that the iron abundance is the same in the disk and in this matter, then this contribution can be inferred from the ratio of the narrow to the total intensity, to be about 1/3.

4.3. The warm absorber

In order to quantify, in the frame of a single zone, equilibrium ionization model, the column N_W and the ionization parameter ξ of the warm absorber, we fitted the data with a model where the four parameters describing the two edges in the BMS are replaced by the two parameters N_W and ξ, and the XSPEC module used is ABSORI. In this module the opacity of the gas is based on the ionization distribution of the relevant atomic species (same abundances as in the module WABS), in a slab of Thomson–thin gas, as a function of the ionization parameter $\xi=L/nR^2$ (erg cm s^{-1}), where n is the number density of the gas and R its distance from the ionizing source with luminosity L in the interval 5 eV to 20 keV. We imposed the spectral slope of this source to be equal to that of the PL. The results of the fit are given in Table 4. We note the improvement in χ^2 with respect to the BMS fit, $\Delta\chi^2$=–2.2 with two less parameters, while the parameters in common, in particular I_k and r, have remained practically unchanged. This means that, although a single zone ionization model may often be an oversimplification (see e.g. Reynolds 1997 and ref. therein), in this observation, perhaps due to the limited statistics in the LECS data as compared to ASCA data, it seems to apply rather well. It must be recognized, though, that ξ turns out to be poorly constrained, likely because of the reciprocal interference of the cold and warm gas columns, which are of comparable thickness. In Fig. 8 the best fit model, deprived for clarity of the contribution by the cold absorbers N_H and N_{Hg}, illustrates the presence of two absorption features corresponding to the two edges detected in the BMS fit, namely a blend of O VI (0.67 keV) and O VII (0.74 keV) edges, and a shallow trough around 1 keV, due to contributions by Fe L and Ne K edges.

Table 4. Fit with a warm absorber (cos i=1)

Γ	$1.88^{+0.04}_{-0.03}$
N_H (10^{21} cm^{-2})[a]	$2.62^{+0.81}_{-1.46}$
N_W (10^{21} cm^{-2})[a]	$3.05^{+1.40}_{-1.04}$
ξ	$2.4^{+24}_{-2.0}$
E_f (keV)	313^{+219}_{-100}
r	$0.59^{+0.16}_{-0.13}$
E_k (keV)[b]	$6.49^{+0.18}_{-0.16}$
σ_k (keV)	$0.36^{+0.29}_{-0.21}$
I_k (10^{-4} cm^{-2} s^{-1})	$1.51^{+0.80}_{-0.53}$
EW_k (eV)	109^{+57}_{-31}
χ^2/d.o.f.	157.7/143

[a] In addition to $N_{Hg}=4.55\times10^{20}$ cm^{-2}
[b] In the source frame

5. Comments and comparison with previous results

We now comment on our results, also in comparison with earlier results as described in papers mentioned in Sect. 2.

If we compare the BMS fit with $i=0^\circ$ (Table 3) with the DISKLINE fits (i=45°–50°), we note that the EW of the iron line turns out to be practically the same, about 110 eV. Adopting the "normal" abundances in Anders & Grevesse (1993), for an $\Omega=2\pi$ geometry the expected EW is 192 eV with $i=0^\circ$ (Matt et al. 1997), or about 165 eV with $i=45^\circ$–50° (Matt et al. 1991). The difference in both cases with respect to the

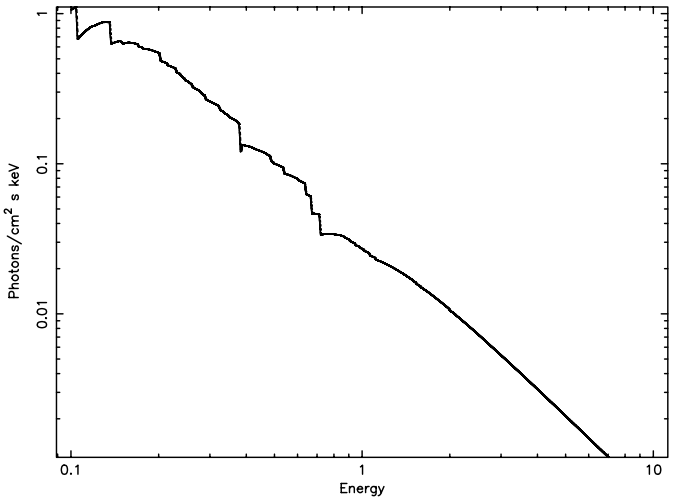

Fig. 8. The best fit model when the two edges in the BMS are replaced by a column of "warm" gas. In this figure the cold absorber contribution is ignored for clarity.

measured value is significant and indicates that Ω is smaller than 2π. This indication is well supported by the estimate of r: this is significantly smaller than one in the BMS fit; in the DISKLINE fit it is only marginally smaller than one, but the contribution to the RC by material giving rise to the narrow line could account for about one third of it, as noted in Sect. 4.2, thus bringing the values of r and EW from the disk in closer agreement. An Ω=2π geometry could be retained by assuming either anisotropy in the primary emission pattern, or time delay in the response of fluorescence and reflection to changes in the continuum, as tentatively found by Fiore et al. (1992).

The average flux in our observation is nearly identical to (30% higher than) the Ginga (ASCA) observations. Comparison with our BMS fit of the similar one performed by Fiore et al. (1992) on the Ginga observation shows a substantial agreement. For a comparison with the ASCA results discussed in Cappi et al. (1996), it is appropriate to report first the outcome of a reanalysis of their best fit model, which is equivalent to our BMS with i=0°, performed with the same tools used by us and the 90% confidence errors for two i.p.: Γ=$1.98^{+0.06}_{-0.09}$, r=$2.58^{+1.23}_{-1.11}$, line EW=87^{+352}_{-42} eV. We note that both Gamma and line EW are within the errors consistent with our results, but that there seems to exist an irreducible discrepancy in the value of r. It is then to be remarked that, within the ample margins of the error on the iron line EW, the evidence of an internal discrepancy with respect to r, noted in Sect. 2, is by no means compelling. Rather, the comparison between the two observations indicates that the intensity of the RC can change both in absolute and in relative terms. The relative changes could be naturally attributed to a delay in the response of the RC to variations in the intensity of the PL, as suggested also by Cappi et al. (1996) to explain the exceptionally large best fit value of r. Their suggestion is made the more plausible by the strong, occasional outbursts of short duration in the ASM/RXTE light curve quoted in Sect. 2.

Concerning the energy of the line, we do not confirm the ASCA evidence in Cappi et al. (1996) that it is redshifted by about 100 eV, their gaussian fit value being 6.30$\pm$0.07, but with the errors in our estimate (6.48$\pm$0.17) we cannot exclude it either. This difference in the gaussian best fit energy, whatever the cause might be, is the most likely cause of the discrepancy in inclination angle, from the DISKLINE fit, between us and Cappi et al. (1996), who find an upper limit of 25° (same as found also by Mushotzky et al. 1995 and by Nandra et al. 1997 with the same observation).

In the ASCA observation Cappi et al. (1996) found clear evidence of two edges coinciding with O VII and O VIII redshifted by about 25 eV. A similar result, albeit different in the estimate of the optical depths, was obtained by Reynolds (1997), who kept the two energies fixed at their atomic values. In the BeppoSAX observation the ionization degree of the absorber was apparently lower, with no significant sign of the O VIII edge. This difference is further borne out by the estimate of the ionization parameter. Both Cappi et al. (1996) and Reynolds (1997) found ξ equal to about 10: we find instead ξ about 2.5 (although admittedly with a large uncertainty), while the best fit values of N_W are comparable. Since the intensity of the source in our observation was 30% higher than in the other, if the strength of the ionizing flux is the driving parameter and is proportional to the intensity of the power law, the reason of the difference between the two epochs must be sought elsewhere. In this respect it is remarkable that both Cappi et al. (1996) and Reynolds (1997) obtain a worse χ^2 with the warm absorber model than with the two edges model. In addition George et al. (1998), which apply to the same observation also more sophisticated models, do not find a single case which passes their acceptability limit based on the χ^2 statistics. This is suggestive of a situation which is either more complex than the single–zone or far from equilibrium. We propose the possibility that at the epoch of the ASCA observation the ionization degree was above average and out of equilibrium, due to a sharp transition from a high state which must have occurred before the start of the observation. Non–equilibrium states are discussed in Nicastro et al. (1999a), which typically require rather sharp transitions in the intensity of the source. This possibility is very attractive, in that it offers simultaneously an explanation for the exceptionally high value of the relative strength of the reflection component in the ASCA data.

Lastly we stress that we have been able for the first time to constrain significantly the energy of the exponential cut–off in the PL. The value we find is close to the lower end of the ample range estimated by Madejski et al. (1995) by combining the simultaneous ROSAT and OSSE (Compton GRO) observation with the best matching (in flux) fraction of the Ginga observation. That estimate, though, is affected by the further uncertainty associated with possible variations in the relative intensity of the reflection discussed above, so is the physical modelling of the same combination of data by Zdziarski et al. (1994). A discussion of the physical implications of our measurement in terms of self–consistent Comptonization models is in progress.

6. Conclusions

The main conclusions we draw from our analysis of this observation of IC4329A, are the following.

a) For the first time the amplitude of the reflection component in this galaxy has been constrained with sufficient accuracy to draw conclusion from the simultaneously measured, and even better constrained, EW of the iron fluorescence line. The values of the two parameters indicate that the geometrical factors entering the matter illumination by the primary, power law photons imply a solid angle substantially less than 2π. A 2π geometry can be retained if either anisotropy in the primary emission or geometrical lags in the response of the reprocessed photons to changes in the primary radiation are deemed likely to occur.

b) The power law is definitely affected by a high energy turnover, which, if modelled as an exponential cutoff, implies an E_f energy of about 270 keV. At present, this is the fourth firm, individual determination of a high energy turnover in Seyfert 1 spectra, after NGC 4151 (Jourdain et al. 1992, Zdziarski et al. 1996, Piro et al. 1998), MCG-6-30-15 (Guainazzi et al. 1999b) and NGC 5548 (Nicastro et al. 1999b).

c) The state of the warm absorber in this observation appears different from that found in the ASCA observation, in particular the absence of a significant absorption at the O VIII K edge implies a lower ionization parameter, which contrasts the fact that the intensity of the ionizing continuum, as inferred from the direct primary emission, is actually 30% higher. We tentatively argue that at the epoch of the ASCA observation the ionization state might have been higher than in equilibrium, due to a transition of the continuum from a high to a low state immediately prior to that epoch. Comfortably this same argument offers an explanation for the strength of the reflection component at the same epoch, which, albeit ill constrained, seems to have been irreducibly higher than found at the epoch of our observation. In other words, the comparison between the BeppoSAX and the ASCA observations is suggestive of delay effects due to geometrical factors in the reflection, and to relaxation to an equilibrium state in the ionization of the absorber.

Acknowledgements. The BeppoSAX satellite is a joint Italian–Dutch program. We wish to thank the BeppoSAX Scientific Data Center for assistance. The work was partially supported by the Italian Space Agency, and by the Ministry for University and Research (MURST) under grant COFIN98–02–32.

References

Anders E., Grevesse N., 1993, Geochim. Cosmochim. Acta 53, 197
Boella G., Butler R.C., Perola G.C., et al., 1997a, A&AS 122, 299
Boella G., Chiappetti L., Conti G., et al., 1997b, A&AS 122, 327
Cappi M., Mihara T., Matsuoka M., et al., 1996, ApJ 458, 149
Elvis M., Lockman F.J., Wilkes B., 1989, AJ 97, 777
Fabian A.C., Nandra K., Celotti A., et al., 1993, ApJ 416, L57
Fiore F., Perola G.C., Matsuoka M., Yamauchi M., Piro L., 1992, A&A 262, 37
Fiore F., Guainazzi M., Grandi P., 1999, SDC report (ftp://www.sdc.asi.it/pub/sax/doc/software_docs/saxabc_v1.2.ps.gz)
Frontera F., Costa E., Dal Fiume D., et al., 1997, A&AS 122, 357
George I.M., Turner T.J., Netzer H., et al., 1998, ApJS 114, 73
Gondek D., Zdziarski A.A., Johnson W.N., et al., 1996, MNRAS 282, 646
Guainazzi M., Perola G.C., Matt G., et al., 1999a, A&A 346, 407
Guainazzi M., Matt G., Molendi S., et al., 1999b, A&A 341, L27
Jourdain E., Bassani L., Buchet L., et al., 1992, A&A 256, L38
Madejski G.M., Zdziarski A.A., Turner T.J., et al., 1995, ApJ 438, 672
Manzo G., Giarrusso S., Santangelo A., et al., 1997, A&AS 122, 341
Matt G., Perola G.C., Piro L., 1991, A&A 247, 25
Matt G., Fabian A.C., Reynolds C.S., 1997, MNRAS 289, 175
Mushotzky R.F., Done C., Pounds K.A., 1993, ARA&A 31, 717
Mushotzky R.F., Fabian A.C., Iwasawa K., et al., 1995, MNRAS 272, L9
Nandra K., Pounds K.A., 1994, MNRAS 268, 405
Nandra K., George I.M., Mushotzky R.F., Turner T.J., Yaqoob T., 1997, ApJ 477, 602
Nicastro F., Fiore F., Elvis M., Perola G.C., 1999a, ApJ 512, 184
Nicastro F., Piro L., Feroci M., et al., 1999b, ApJ submitted
Parmar A.N., Martin D.D.E., Bavdaz M., et al., 1997, A&AS 122, 309
Petre R., Mushotzky R.F., Krolik J., Holt S.S., 1984, ApJ 280, 499
Pierre M., Bohringer H., Ebeling H., et al., 1994, A&A 290, 725
Piro L., Yamauchi M., Matsuoka M., 1990, ApJ 360, L35
Piro L., Nicastro F., Feroci M., et al., 1998, Nucl. Phys. B (Proc. Suppl.) 69, 481
Reynolds C.S., 1997, MNRAS 286, 513
Walter R., Fink H., 1993, A&A 274, 105
Wandel A., Peterson B.M., Malkan M.A., 1999, ApJ in press
Whittle M., 1992, ApJS 79, 49
Wilson A.S., Penston M.V., 1979, ApJ 232, 389
Zdziarski A.A., Fabian A.C., Nandra K., et al., 1994, MNRAS 269, L55
Zdziarski A.A., Johnson W.N., Done C., Smith D., McNaron-Brown K., 1995, ApJ 438, L63
Zdziarski A.A., Johnson W.N., Magdziarz P., 1996, MNRAS 283, 193